

Precision Measurement of the Photon Recoil of an Atom Using Atomic Interferometry

David S. Weiss,^(a) Brenton C. Young, and Steven Chu

Physics Department, Stanford University, Stanford, California 94305

(Received 2 February 1993)

The atomic recoil from the absorption of up to 60 photons is measured using an atom interferometer. We determine \hbar/m_Cs with a precision of 10^{-7} in 2 h of integration time.

PACS numbers: 35.10.Fk, 32.80.Pj, 35.10.Bg

The photon recoil of an atom was first observed spectroscopically in the doubling of certain spectral peaks in saturation spectroscopy [1]. The authors pointed out that the frequency splitting of these peaks is proportional to \hbar/m , allowing the possibility of a precision measurement. We describe a new method of measuring \hbar/m based on recent advances in laser cooling [2] and atom interferometry with Raman transitions [3].

The significance of \hbar/m lies in the fact that mass appears in quantum mechanical equations only in that ratio, so that tests of quantum theories typically require only knowledge of \hbar/m , and not of m . As a particularly important example, the fine structure constant α is determined by combined measurements of \hbar/m_e and the Rydberg constant R_∞ ,

$$\alpha^2 = \frac{2R_\infty}{c} \frac{\hbar}{m_e}.$$

Many mass ratios can be measured to high precision, so that the particular mass in the ratio \hbar/m is of secondary importance [4,5]. Recently \hbar/m_n has been measured with an accuracy of 8×10^{-7} by diffracting neutrons with a silicon crystal [6]. We now report a measurement of \hbar/m_Cs to a precision of 10^{-7} . It is hoped that future versions of this experiment will determine α to better accuracy than can currently be obtained independently of the $g-2$ experiment and theory [7].

The basic physical principle of this atomic recoil velocity measurement does not depend on atomic interference. Figure 1(a) shows the center of mass of an atom with zero horizontal velocity in the laboratory frame which absorbs a photon from a rightward propagating laser beam tuned on resonance. To conserve momentum its velocity changes by $\hbar k/m$. It is then deexcited by a photon from a leftward propagating beam. The deexcitation and excitation frequencies are separated by $\Delta\omega = 2\hbar k^2/m$ so that accurate measurements of $\Delta\omega$ and the photon wavelength [8] determine \hbar/m .

This simple experiment is not optimal because it forgoes the advantages of Ramsey spectroscopy, which include increased resolution, larger signal, and reduced systematic shifts. An improved version shown in Fig. 1(b) replaces each π pulse with two $\pi/2$ pulses. Optical Ramsey spectroscopy uses this same pulse sequence, which puts the atom in a superposition of eight trajectories, two pairs of which interfere when the spacing within the $\pi/2$

pulse pairs is equal [9,10]. The crucial difference between the two interfering pairs is that their velocities differ by two photon recoils, so that the center frequencies of the sets of Ramsey fringes they produce are displaced by $2\hbar k^2/m$. The atom's initial velocity, the acceleration due to gravity, and all position-independent frequency shifts do not affect the recoil shift measurement.

We have improved the optical Ramsey experiment in three basic ways. First, the transitions are between hyperfine ground states via a Doppler-sensitive stimulated Raman transition [11]. The recoils from the absorbed

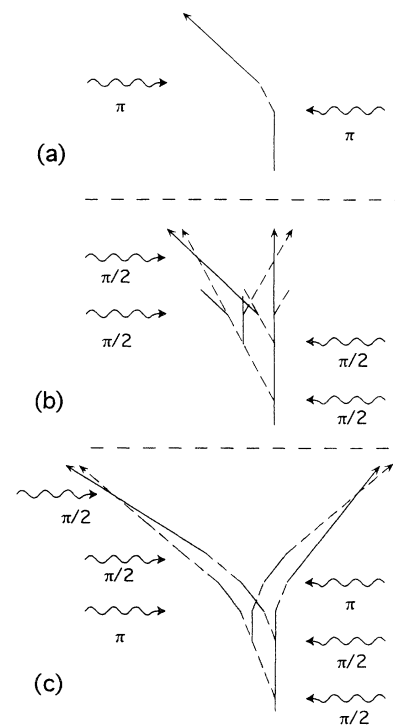


FIG. 1. Wave packet trajectories for photon recoil measurements. The solid and dashed lines correspond to the two internal states of the atom. The photon arrows show the direction of the effective k vector for velocity-selective stimulated Raman transitions. (a) The simplest photon recoil measurement. (b) The basic double atom interferometer sequence. The four paths which do not interfere at the final $\pi/2$ pulse are truncated for clarity. (c) The double interferometer with two additional π pulses. Currently up to 15 π pulses are used.

and emitted photons in this transition are in the same direction, so the effective k vector is $k_{\text{eff}} = k_1 + k_2$. Also, we need only control the difference frequency between two laser beams, not their absolute frequency, yielding all the convenience and power of microwave measurements. These Raman transitions simulate a microwave transition where the photon carries an ultraviolet recoil kick. Second, since both atomic levels are ground states, the linewidth of the stimulated Raman transition is limited only by the measurement time, which can be quite long in an atomic fountain. Third, we add to our interferometer up to 15π pulses with alternating propagation directions, sandwiched between the middle two $\pi/2$ pulses [see Fig. 1(c)]. Each π pulse adds an ultraviolet photon recoil to each atomic path, so that for $N \pi$ pulses the separation between the two sets of interference fringes is multiplied by $N+1$. In this manner we have separated the two interferometer end points by over 4 mm.

Laser cooled atoms and atomic interferometers have great promise for a broad range of sensitive measurements, but no previous experiment using either of these new technologies has measured a fundamental constant to high precision. Because \hbar/m is already known to high accuracy, our measurement is well suited for studying systematic errors in light-pulse interferometers.

The apparatus is similar to previous atomic fountain experiments (see Fig. 2) [12]. A beam of thermal Cs atoms is slowed and loaded into a magneto-optic trap (MOT) [13]. In 0.2 s, $\sim 5 \times 10^8$ atoms are loaded before the trapping magnet is shut off, leaving the atoms to equilibrate in optical molasses. The molasses beam fre-

quencies are then acousto-optically shifted to create molasses in a frame moving upwards, $\sim 5^\circ$ off vertical at 2 m/s. [14]. The light intensity is then decreased to cool the atoms to $\sim 3.5 \mu\text{K}$, after which a mechanical shutter blocks the light, leaving the atoms on a ballistic trajectory upward. The repetition rate of the experiment is 2 Hz.

On their way up most of the atoms are optically pumped into the $F=4$, $m_F=0$ magnetic sublevel. Then a velocity-selective Raman beam pair, which propagates along the 85 mG bias magnetic field axis, transfers a group of atoms with a velocity width of $\sim 500 \mu\text{m/s}$ into the $F=3$, $m_F=0$ level. A beam resonant with the $6S_{1/2}$, $F=4$ to $6P_{3/2}$, $F=5$ cycling transition pushes away the remaining $F=4$ atoms, while the selected atoms continue upward. Near the top of the trajectory, a single pair of Raman beams, parallel to the previous Raman beams, delivers all of the interferometer pulses.

The Raman beams are generated by two diode lasers which are phase locked to each other with a 9.2 GHz frequency difference [15]. The lock reference frequency is the summed output of two precision oscillators, one a digital synthesizer which controls the Raman beam difference frequency. The beams are combined, sent through an acousto-optic modulator for intensity control, and coupled into a single mode optical fiber to ensure precise overlap. The final beams have 15 mW total power in a 2.3 cm Gaussian diameter, and are frequency locked between 0.5 and 2.5 GHz from the $6P_{3/2}$ state. The maximum Rabi frequency of the interferometer pulses is ~ 10 kHz. The interferometer Raman beams are retro-reflected from a mirror mounted on a precision air rail, which isolates it from residual horizontal vibrations of the vibration isolated table. Both Raman beam frequencies travel in both directions, but the velocity along the beam is made large enough so that only one of the two Doppler-sensitive pairs is resonant at any time, and the Doppler-free pairs and standing wave pairs are not resonant with the atoms.

The frequency width of each interferometer pulse is narrower than the recoil shift, so a given sequence of pulse frequencies is only resonant with one pair of interfering paths. Atoms which branch off into non-resonant paths, either because they are in the other interferometer paths or because of imperfect π pulses, contribute a background which reduces fringe contrast. Most of these atoms can be removed because both paths in any given interferometer are in the same atomic state during the time between the $\pi/2$ pulse pairs. Therefore, before and after the last π pulse, we pulse on one of two clearing beams aligned nearly parallel to the interferometer beams. $F=3$ atoms are cleared by a linearly polarized beam resonant with the $F=2$ excited state, and $F=4$ atoms by a beam resonant with the $F=5$ excited state.

After the interferometer sequence, the remaining atoms fall back down through the probe/blasting beam. Fluorescence from $F=4$ atoms is detected with a pho-

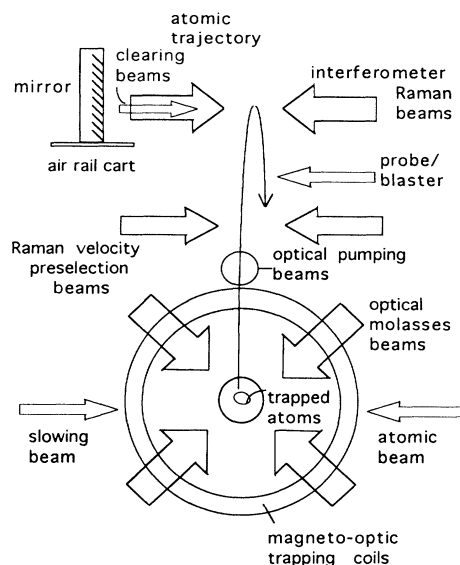


FIG. 2. Schematic of the experiment. Cs atoms trapped in a MOT are launched on a ballistic trajectory. The number of atoms in the two hyperfine ground states are detected by fluorescence as the atoms fall through the probe/blaster beam.

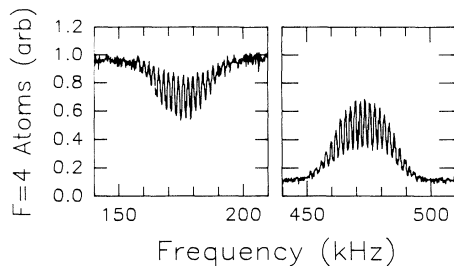


FIG. 3. Ramsey fringe recoil doublet. The separation between $\pi/2$ pulses is reduced to 1 ms to reveal the coarse signal structure. The frequency of the first two $\pi/2$ pulses is the same for both sets of fringes, but the frequencies of the 8 π pulses are different. Only the frequency of the final two $\pi/2$ pulses is scanned.

tomultiplier tube, as the atoms are pushed out of resonance by the unidirectional beam. In 2 ms, fluorescence from $F=4$ atoms nearly vanishes, while the $F=3$ atoms have fallen only a fraction of a probe beam diameter. A beam resonant with the $F=3$ to $F=4$ transition then optically pumps the $F=3$ atoms into the $F=4$ state and the probe excites them with nearly equal efficiency as the original $F=4$ atoms. The fluorescence ratio allows us to normalize the signal [16].

Illustrative data with 1 ms between $\pi/2$ pulses (within each pair) are shown in Fig. 3. The $\pi/2$ pulse separation was typically 15 to 20 ms. The two sets of fringes correspond to the two interferometers in Fig. 1(c). The off-resonant baselines on the left and right in Fig. 3 differ because before the final $\pi/2$ pulses, the atoms are either in the $F=4$ state, $N+1$ recoil kicks away from the pre-selected velocity, or in the $F=3$ state, $N+1$ recoil kicks in the opposite direction. The fringes at the Rabi peak do not extend to the baseline because half of the atoms that survive the clearing are necessarily in two noninterfering trajectories. Although the broad structure of the signal is inverted for the two interferometers, the fringe pattern is not.

Alternate data points are taken from the two interferometers as the frequency of the final $\pi/2$ pair is scanned. Least-squares fits of the interference patterns to sinusoids yield the recoil splitting to within an integer multiple of the fringe frequency. Scans with different $\pi/2$ pulse separations determine the correct fringe number. Figure 4 shows a fringe pattern taken in 1 min with 18 ms between $\pi/2$ pulses and 10 π pulses. In 2 h we can measure the photon recoil with a relative precision of 10^{-7} .

We have studied the systematic errors in this experiment. A more detailed discussion of anticipated and measured limits on systematic errors appears in Ref. [17], and will be published in a longer paper. The most important experimental handles on systematic errors are the time between $\pi/2$ pulses (T), number of π pulses (N), Raman laser detuning from the excited state (Δ), and

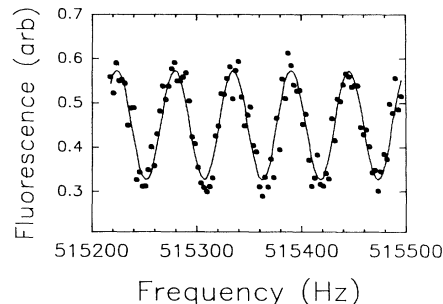


FIG. 4. Typical interference fringe pattern. This is 1 min of data showing the central fringes of one of the interferometers. There are 18 ms between each $\pi/2$ pulse pair and 10 intermediate π pulses, so the frequency separation from the other set of Ramsey fringes is $22\hbar(k_1+k_2)^2/m=363$ kHz.

Rabi frequency (Ω). Using these experimental “knobs,” we have uncovered and removed several errors at the 10^{-6} level. The largest systematic error was caused by optical standing waves from retroreflected, linearly polarized Raman beams. These standing waves shift the measurement as a function of the distance of the interferometer from the retroreflecting mirror. Switching to $\sigma^+\sigma^-$ polarizations eliminated the standing waves and this shift.

Magnetic field gradients shift the phases of the interferometers differently, and will alter the measured recoil. We monitor this shift in two ways. First, we reverse the direction of all the Raman pulses, which creates interference paths that are mirror symmetric to the original ones. Since the two paths in each interferometer flip sides, the shift from any linear gradient reverses. Second, we change the parity of the number of π pulses, which changes the internal state during the time between the last two $\pi/2$ pulses for all the paths. Increasing the bias magnetic field fourfold causes a 1 ppm shift in the measured recoil that reverses sign in just this manner. With our typical bias field, these reversals do not affect our measurement.

We have also looked for dependences on beam alignment Δ , the relative ac Stark shifts of the hyperfine levels, and clearing beam power. Our current empirical limits on shifts due to these effects are at the 0.25 ppm level. Although we do not see a clear dependence on T , Δ , or N , our measured value is 8.5×10^{-7} below the accepted value, which has a relative uncertainty of 7.7×10^{-8} .

We believe the cause of this presumed error is wave front distortion from imperfect optics. In the past we have seen repeatable changes in the measured recoil of up to 10 ppm with our routine reversals, at about the same level as the disagreement with the accepted value. Successive improvements in the optics have led to measured recoils progressively closer to the accepted value, with progressively smaller internal inconsistencies. Still, in the current configuration it is difficult to ensure that all effects due to wave front distortion have been eliminated.

The next improvement in this experiment is to orient

the Raman beams vertically. The effects of wave front distortions will be easier to study in this configuration because the transverse motion of atoms in the beams can be varied. Also, we will be able to easily vary where along the beam atoms receive interferometer pulses, and the $\pi/2$ - π - $\pi/2$ pulse interferometer will provide extra information on the effects of wave front distortion. The frequencies of the Raman beams will have to be adjusted between each pulse to account for gravitational acceleration, but the adjustment is the same for the two interferometers apart from a slight difference in the local gravitational acceleration. Furthermore, the vertical launch should permit a 200 ms $\pi/2$ pulse separation and give time for additional π pulses. We anticipate a resolution of 10^{-9} in 1 h, but it is difficult to now predict the severity of the associated systematic errors, particularly those related to the quality of the Raman beams. However, the simplicity of this system, which fundamentally depends only on simple interactions between free atoms and photons, makes the prospects for accuracy in this and similar measurements promising.

We thank Kurt Gibble and Mark Kasevich for useful discussions, and Barry Taylor for pointing out the role of \hbar/m in the determination of α . B.C.Y. was supported by an NSF Fellowship. This work was funded in part by the AFOSR and NSF.

^(a)Present address: Ecole Normale Supérieure, 24 rue Lhomond, 75231 Paris CEDEX 05, France.

[1] J. L. Hall, C. J. Borde, and K. Uehara, Phys. Rev. Lett.

- 37, 1339 (1976).
 [2] S. Chu, Science **253**, 861 (1991).
 [3] M. Kasevich and S. Chu, Phys. Rev. Lett. **67**, 181 (1991); Appl. Phys. B **54**, 321 (1992).
 [4] J. R. S. Van Dyck, F. L. Moore, D. L. Farnham, and P. B. Schwinberg, Int. J. Mass Spectrom Ion Processes **66**, 327 (1985).
 [5] A. H. Wapstra, G. Audi, and R. Hoekstra, Atomic Data Nucl. Data Tables **39**, 290 (1988).
 [6] A. G. Klein, G. I. Opat, and W. A. Hamilton, Phys. Rev. Lett. **50**, 563 (1983).
 [7] *Quantum Electrodynamics*, edited by T. Kinoshita (World Scientific, Singapore, 1990).
 [8] G. Avila, P. Gain, C. E. De, and P. Cerez, Metrologia **22**, 111 (1986).
 [9] C. J. Bordé *et al.*, Phys. Rev. A **30**, 1836 (1984).
 [10] G. Hennig *et al.*, in *Laser Spectroscopy X*, edited by M. Ducloy, E. Giacobino, and G. Camys (World Scientific, Teaneck, NJ, 1992).
 [11] M. Kasevich *et al.*, Phys. Rev. Lett. **66**, 2297 (1991).
 [12] M. A. Kasevich, E. Riis, S. Chu, and R. G. DeVoe, Phys. Rev. Lett. **63**, 612 (1989).
 [13] E. L. Raab, M. Prentiss, A. Cable, S. Chu, and D. E. Pritchard, Phys. Rev. Lett. **59**, 2631 (1987).
 [14] D. S. Weiss, E. Riis, M. A. Kasevich, K. A. Moler, and S. Chu, in *Light Induced Kinetic Effects on Atoms, Ions, and Molecules*, edited by I. Moi, S. Gozzini, C. Gabbanini, E. Arimondo, and F. Strumias (ETS Editrice, Pisa, 1991), p. 35.
 [15] S. Swartz, J. L. Hall, K. E. Gibble, and D. S. Weiss (to be published).
 [16] C. Monroe, H. Robinson, and C. Wieman, Opt. Lett. **16**, 50 (1991).
 [17] D. S. Weiss, Ph.D. thesis, Stanford, 1993.